

1 **Structural and transcriptional evidence of mechanotransduction in the**  
2 ***Drosophila suzukii* ovipositor**

3 **Cristina Maria Crava<sup>1\*@</sup>, Damiano Zanini<sup>2#</sup>, Simone Amati<sup>1</sup>, Giorgia Sollai<sup>3</sup>, Roberto Crnjar<sup>3</sup>,**  
4 **Marco Paoli<sup>2</sup>, Marco Valerio Rossi-Stacconi<sup>1</sup>, Omar Rota-Stabelli<sup>1</sup>, Gabriella Tait<sup>1</sup>, Albrecht**  
5 **Haase<sup>2</sup>, Roberto Romani<sup>4\*a</sup>, Gianfranco Anfora<sup>1,5a</sup>**

6 <sup>1</sup>Research and Innovation Centre, Fondazione Edmund Mach, San Michele all'Adige, Italy

7 <sup>2</sup>Center for Mind/Brain Sciences and Department of Physics, University of Trento, Rovereto, Italy

8 <sup>3</sup>Department of Biomedical Sciences, Section of Physiology, University of Cagliari

9 <sup>4</sup>Department of Agricultural, Food and Environmental Sciences, University of Perugia, Perugia, Italy

10 <sup>5</sup>Centre Agriculture, Food and Environment (C3A), University of Trento, San Michele all'Adige,  
11 Italy

12 <sup>a</sup>Authors share joint seniority

13 **\* Correspondence:**

14 Maria Cristina Crava  
15 m.cristina.crava@uv.es

16 Roberto Romani  
17 roberto.romani@unipg.it  
18

19 **CURRENT ADDRESSES:**

20 @ ERI BIOTECMED, University of Valencia, Burjassot, Spain

21 # Neurobiology and Genetics, Biocenter, University of Würzburg, Würzburg, Germany

22

23 **ABSTRACT**

24 *Drosophila suzukii* is an invasive pest that prefers to lay eggs in ripening fruits, while most closely  
25 related *Drosophila* species exclusively use rotten fruit as oviposition substrates. This behaviour is  
26 allowed by an enlarged and serrated ovipositor that can pierce intact fruit skin, and by multiple contact  
27 sensory systems (mechanosensation and taste) that detect the optimal egg-laying substrates. Here, we  
28 tested the hypothesis that bristles present in the *D. suzukii* ovipositor tip contribute to these sensory  
29 modalities. Analysis of the ultrastructure revealed that four different types of cuticular elements  
30 (conical pegs type 1 and 2, chaetic and trichoid sensilla) are present on the tip of each ovipositor  
31 plate. All of them have a poreless shaft and are innervated at their base by a single neuron that ends  
32 in a distal tubular body, thus resembling mechanosensitive structures. Fluorescent labelling in *D.*  
33 *suzukii* and *D. melanogaster* revealed that pegs located on the ventral side of the ovipositor tip are  
34 innervated by a single neuron in both species. RNA-sequencing profiled gene expression of the  
35 terminalia of *D. suzukii* and of three other *Drosophila* species with gradual changes in their ovipositor  
36 structure (from serrated to blunt ovipositor: *Drosophila subpulchrella*, *Drosophila biarmipes* and *D.*  
37 *melanogaster*). Our results revealed few species-specific transcripts and an overlapping expression  
38 of candidate mechanosensitive genes as well as the presence of some chemoreceptor transcripts.  
39 These experimental evidences suggest a mechanosensitive function for the *D. suzukii* ovipositor,  
40 which might be of evolutionary importance across *Drosophila* species independently from ovipositor  
41 shape.

42

43

44 **KEYWORDS**

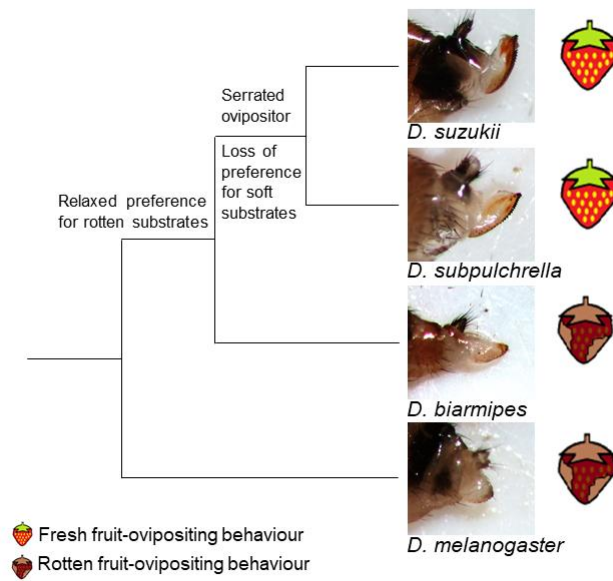
45 Spotted wing drosophila, mechanosensitive bristles, ultrastructure, comparative RNA-seq

46

## 47 **INTRODUCTION**

48 *Drosophila suzukii* (Matsumura) (Diptera: Drosophilidae), also called spotted wing drosophila, is an  
49 invasive South Eastern Asian fly species that was identified outside its native range in California in  
50 2008, and in Spain and Italy in 2009 (Cini et al., 2012; Hauser, 2011). Since then, it has spread quickly  
51 across several countries in both continents, where it is now a major threat for soft fruit production  
52 (Asplen et al., 2015). Differently from the majority of drosophilids, which thrive and lay eggs on  
53 already damaged or rotting vegetal substrates, *D. suzukii* can pierce and lay eggs on healthy ripening  
54 fruits before harvesting. Wherever it is present, this causes extensive agricultural damage and has  
55 boosted research on the ecology and chemosensory behaviour of *D. suzukii* with the aim to find  
56 innovative, effective, and eco-friendly methods to reduce its attacks (reviewed in (Cloonan et al.,  
57 2018)).

58 Several aspects of *D. suzukii* ecology and genetics have been analysed in a comparative  
59 framework across *Drosophila* species to identify key evolutionary innovations that allowed the  
60 transition from rotten to fresh fruit egg-laying behaviour (Atallah et al., 2014; Crava et al., 2016;  
61 Green et al., 2019; Hickner et al., 2016; Karageorgi et al., 2017; Muto et al., 2018; Ramasamy et al.,  
62 2016). The major morphological shift from rotten fruit-ovipositing *Drosophila* species (like the insect  
63 model *Drosophila melanogaster*) to fresh fruit-ovipositing species (*D. suzukii*) is the presence of an  
64 unusually enlarged and serrated ovipositor. Such structure is shared with the sister species *Drosophila*  
65 *subpulchrella* and allows the wounding of the intact skin of berries (Figure 1) (Atallah et al., 2014).  
66 This feature is not present in another closely related Asiatic spotted wing *Drosophila* species,  
67 *Drosophila biarmipes*, whose ovipositor shows intermediate features between *D. suzukii* and *D.*  
68 *melanogaster* (Figure 1) (Atallah et al., 2014). The ovipositor morphology correlates with the  
69 stiffness of the oviposition substrates, and serrated design facilitates egg-laying by attenuating the  
70 penetration force required to cut through the fruit skin; accordingly, *D. melanogaster* egg-laying is  
71 inhibited by stiff substrates, whereas *D. suzukii* has a broad tolerance, and *D. biarmipes* displays an  
72 intermediate behaviour (Karageorgi et al., 2017).



74

75 **Figure 1 Evolutionary affinities and ovipositor shapes of *Drosophila suzukii* and other *Drosophila* species**  
 76 **used in the study.**

77 The currently most accepted scenario for fresh fruit-egg laying behaviour evolution (Karageorgi et al.,2017).

78 Phylogeny is based on Atallah et al. (2014).

79

80 To detect substrate stiffness, insects rely on mechanosensitive receptors. In *Drosophila* spp.,

81 mechanosensitive organs are scattered throughout the body and can be of different type such as

82 bristles, hair plates, campaniform sensilla, and chordotonal organs (Karkali and Martin-Blanco,

83 2017). Bristles are the main touch receptors, while the other three organs are proprioceptors, *i.e.*

84 mechanosensitive structures that monitor the positions, and relative movements of the fly's own body

85 parts (Keil and Steinbreicht, 1984; Tuthill and Wilson, 2016). A feature common to all

86 mechanosensitive sensilla is the presence of mechanosensitive neurons (MNs), which have an outer

87 dendritic segment that ends in a distal tubular body in contact with the flexible base of the sensillum

88 shaft (Walker et al., 2000). Pure mechanosensitive sensilla accommodate a single MN whereas in

89 poly-innervated taste sensilla the MN is coupled with multiple gustatory neurons and four non-neural

90 cells (trichogen cell, tormogen cell, thecogen cell and glial cell) (Falk et al., 1976; Stocker, 1994).

91 While the tip of mono-innervated mechanosensitive sensilla is smooth, the one of taste sensilla has

92 one or few pores that allow dendrites of gustatory neurons to get in contact with external fluid (Falk  
93 and Atidia, 1975). In *D. melanogaster*, poly-innervated taste sensilla have been found in the labial  
94 palps, the pharynx, the legs and the wings, and their presence on the external genitalia was suggested  
95 (Stocker, 1994). In *D. suzukii*, a single study describes the external morphology of the ovipositor tip  
96 (Atallah et al., 2014), but no information on the ultrastructure of sensilla and pegs (which would  
97 provide clues for the physiological function of these structures) are available yet. Beside  
98 mechanosensation, also the assessment of the chemical composition of the oviposition substrate  
99 contributes to egg-laying behaviour in insects (Aranha and Vasconcelos, 2018). Accordingly,  
100 experiments with transgenic *D. suzukii* impaired in olfaction showed that they preferred ripe over  
101 rotten strawberry puree as wild-type flies when allowed to get in touch with the oviposition substrate  
102 (Karageorgi et al., 2017); thus in *D. suzukii* the contact chemosensory system (*i.e.* taste) is involved  
103 in the process for selecting the optimal egg-laying site, together with mechanosensation. Since the *D.*  
104 *suzukii* ovipositor pierces the fruit skin and comes into contact with fruit flesh, we hypothesize that  
105 this organ may carry taste sensilla, which contribute to the egg-laying decision. Alternatively, it is  
106 possible that *D. suzukii* ovipositor carries pure mechanosensitive sensilla, which may transfer  
107 information on the substrate stiffness and roughness, and on whether the ovipositor has penetrated it.

108 To select among these hypotheses, we analysed the ultrastructure of the pegs and sensilla  
109 present on *D. suzukii* ovipositor tip. We then used fluorescent antibody and GAL4 drivers to label  
110 neurons reaching these structures in both *D. suzukii* and *D. melanogaster*. Lastly, we performed RNA-  
111 seq experiment to understand if terminalia gene expression overlaps among *Drosophila* species  
112 characterised by gradual changes in their ovipositor structure (from blunt to serrated ovipositor)  
113 (Figure 1). Our results reveal the presence of mechanosensitive organs in *D. suzukii* ovipositor and  
114 suggest that mechanotransduction in ovipositor is conserved among *Drosophila* species  
115 independently from ovipositor shape.

## 116 **METHODS**

### 117 *Insects*

118 Insects used for transcriptomics, immunohistochemistry, and electron microscopy were taken from  
119 laboratory colonies maintained at the Fondazione Edmund Mach, S. Michele all'Adige (Italy).  
120 *Drosophila suzukii* and *D. melanogaster* strains were founded with individuals collected in 2010 in  
121 the Trento province (Italy) and periodically refreshed with insects caught from the same field sites.  
122 *Drosophila biarmipes* (genotype Dbii\wild-type, stock # 14023-0361.09) and *D. subpulchrella*  
123 (Dspc\wild-type, stock # 14023-0401.00) strains were obtained from the Drosophila Species Stock  
124 Center (San Diego, CA, US) in 2011. The four *Drosophila* species were reared on a standard diet  
125 ([https://stockcenter.ucsd.edu/info/food\\_cornmeal.php](https://stockcenter.ucsd.edu/info/food_cornmeal.php)), maintained at 23–25 °C, 65 ± 5% relative  
126 humidity, and under a 16:8 h light:dark photoperiod.

127 *Drosophila melanogaster* transgenic strains used for imaging were obtained from the  
128 Bloomington Drosophila Stock Center (BDSC) (Bloomington, IN, US) and reared under the same  
129 conditions as described above.

### 130 ***Drosophila suzukii* ovipositor scanning electron microscopy**

131 Adult females of *D. suzukii* were anaesthetized by exposure to cold temperatures (-18°C) until death,  
132 then they were immediately soaked in 60% alcohol. The ovipositor of each individual was dissected  
133 from the abdomen. Specimens were dehydrated in a series of graded ethanol, from 60% to 99%, 15  
134 min for each step. After dehydration, 99% ethanol was substituted with pure HMDS  
135 (Hexamethyldisilazane, Sigma-Aldrich) and the specimens were allowed to dry under a hood at room  
136 temperature (RT); this step was repeated twice. Up to five samples were mounted on aluminium stubs,  
137 with different orientations, in order to obtain a clear view on the ventral and lateral sides of the  
138 ovipositor. Mounted specimens were gold-sputtered using a Balzers Union SCD 040 unit. The  
139 observations were carried out using a Philips XL 30 scanning electron microscope (SEM) operating  
140 at 7-10 KV, working distance 9-10 mm.

141 ***Drosophila suzukii ovipositor transmission electron microscopy***

142 Ten *D. suzukii* female individuals were anesthetized by exposure to cold temperatures (-18°C) for 60  
143 s, then immediately immersed in a solution of glutaraldehyde and paraformaldehyde (PFA) 2.5% in  
144 0.1 M cacodylate buffer (pH 7.2-7.3) plus 5% sucrose. The ovipositor was detached from the  
145 abdomen, reduced in size to help fixative penetration, and left at 4°C for 24 h. Then, the specimens  
146 were washed twice in cacodylate buffer for 10 min, post-fixed in 1% OsO<sub>4</sub> for 1 h at 4°C, and rinsed  
147 in the cacodylate buffer. They were dehydrated in graded ethanol series from 60% to 99% and  
148 embedded in Epon-Araldite with propylene oxide as bridging solvent. Thin sections were taken with  
149 a diamond knife on an LKB Bromma ultramicrotome and mounted on formvar-coated 50 mesh grids.  
150 Then, sections on grids were stained with uranyl acetate (20 min, RT) and with lead citrate (5 min,  
151 RT). Finally, the sections were imaged with a Philips EM 208 transmission electron microscopy  
152 (TEM). A digital camera MegaViewIII (SIS) provided high-resolution images.

153 ***Drosophila suzukii ovipositor immunohistochemistry***

154 *Drosophila suzukii* adult females were anesthetized using CO<sub>2</sub>. Abdominal distal tips were cut with  
155 a razor blade and fixed in 4% PFA in phosphate-buffered saline (PBS, pH 7.4) (Sigma-Aldrich) for  
156 40 min on ice. Samples were then washed three times with PBS for 20 min, incubated in 10% sucrose  
157 (Sigma-Aldrich) solution, and kept rotating for 1 h at RT. Sucrose solution was increased to 25%,  
158 and samples were kept rotating overnight at 4°C. Samples were then embedded in OCT (OCT  
159 mounting medium Q PATH, VWR), and mounted on a sample holder. Sections of 15 µm thickness  
160 were cut with a CM 1510-3 cryostat (Leica) and collected on a SuperFrost glass slide (ThermoFisher  
161 Scientific). Slides were washed in PBS-T (PBS + 0.1% Triton-X-100, Sigma-Aldrich) for 5 min, and  
162 then blocked in 5% normal goat serum (Sigma-Aldrich) in PBS-T for 30 min. Anti-horseradish  
163 peroxidase (HRP) cyanine-conjugated antibodies (Cy3 AffiniPure Rabbit Anti-HRP, Jackson  
164 ImmunoResearch) diluted 1:300 were used to stain the neurons. Slides were kept in a moist chamber  
165 at 4°C overnight in dark. The next day, antibodies were removed, and the slides were washed three  
166 times with PBS-T for 5 min and then mounted using Vectashield (Vector Laboratories).

167 ***Examination of GAL4-driven GFP expression patterns in the D. melanogaster ovipositor***

168 The native GFP signal was observed at the level of the ovipositor of females expressing the super  
169 bright 6xGFP UAS-reporter (UAS-6xGFP; BDSC accession number 52262) under the pattern of the  
170 pan-neuronal nsyb-GAL4 driver (GMR57C10-GAL4; BDSC accession number 39171). Flies were  
171 anesthetized using CO<sub>2</sub>, abdominal distal tips were cut, embedded in 70% glycerol and immediately  
172 imaged.

173 **Confocal imaging**



174 Images were acquired using a Leica TCS SP8 confocal microscope, equipped with HC PL FLUOTAR  
175 20x/0.55 DRY and HC PL APO CS2 63x/1.40 OIL objectives. For *D. sukuzii*, Cy3 excitation was  
176 performed using a 522-nm solid-state laser, and fluorescence was detected at 561-591 nm. Single  
177 images of 1024 × 1024 pixels (pixel size of 0.072 × 0.072 μm) and stacks with z-steps of 2 μm were  
178 acquired. For *D. melanogaster*, GFP excitation was performed using a 488-nm solid-state laser, and  
179 fluorescence was detected at 499-524 nm. Stacks of 1024 × 1024 pixels (pixel size of 0.06 × 0.06 μm)  
180 optical section were generated with a z-interval of 2 μm. Images were analyzed using Fiji-ImageJ  
181 software (Schindelin et al., 2012).

### 182 ***RNA extraction and sequencing***

183 RNA was extracted from the terminalia of 3- to 10-day old mated females. Dissection was done with  
184 forceps and included both the genitalia and the analia (Supplementary Figure S1). Dissected tissues  
185 were stored at -80 °C in RNAlater (ThermoFisher Scientific) until extraction. Each species sample  
186 was composed of RNA extracted from around 60-80 individuals. Samples were homogenized using  
187 TissueLyser (Qiagen) and total RNA was extracted with TRIzol reagent (ThermoFisher Scientific),  
188 following the manufacturer's protocol. DNA contamination was removed with a DNase I  
189 (ThermoFisher Scientific) incubation step. A second RNA extraction with PureLink RNA Mini Kit  
190 (ThermoFisher Scientific) was performed to remove DNase and to concentrate samples. The total  
191 RNA (~1 μg/sample) was sent to Beckman Coulter Genomics (Danvers, MA USA) for library  
192 preparation and Illumina sequencing. Library preparation was carried out through polyA + selection,  
193 and paired-end (PE) sequencing was run on an Illumina HiSeq 2500 System with V3 chemistry that  
194 generated 100 bp reads. Raw reads are accessible from the Genbank SRA database (BioProject  
195 number PRJNA526247) (Supplementary Table S1).

### 196 ***De novo transcriptome assembly, annotation, and gene ontology***

197 Raw reads were trimmed with Trimmomatic (Bolger et al., 2014). Both paired and unpaired reads  
198 were used for a *de novo* assembly of the transcriptome for each species with Trinity v2.0.6 (Grabherr

199 et al., 2011), using the normalization step and flag `--min_kmer_cov 2`. The transcriptome quality was  
200 checked by mapping the paired reads against the assembled transcriptome with Bowtie2 with default  
201 parameters (Langmead and Salzberg, 2012). The four transcriptomes were annotated using  
202 Standalone Blast+. Blast searches were run with the command `blastx` using the predicted proteins  
203 from the *D. melanogaster* genome (version r6.25) as the database. The top hit for each sequence was  
204 retained when the E-value was less than  $1 \times 10^{-10}$ . PANTHER version 14.0 (Mi et al., 2017) was used  
205 to extract gene ontology (GO) terms (Panther GO-Slim) for each annotated transcriptome. Venn  
206 diagrams were created using Venny 2.1.0 (Oliveros, 2015).

207         Annotation of mechanosensory channels described in *D. melanogaster* have been performed  
208 with iterative `blastx` searches against *D. suzukii* (accession number AWUT000000000) and *D.*  
209 *biarmipes* genomes (accession number AFFD000000000) using *D. melanogaster* sequences as query.  
210 The intron–exon structure was manually determined using BioEdit (Hall, 1999) and full-length  
211 coding sequences were extracted. Quantification of mechanosensory channel expression as well as  
212 of chemoreceptor genes, which we previously annotated in *D. suzukii* and *D. biarmipes* (Crava et al.,  
213 2016; Ramasamy et al., 2016) was done mapping reads to the gene set for each species except for *D.*  
214 *subpulchrella*, where we use the gene set from its sister-species *D. suzukii*. Mapping was performed  
215 with Bowtie2 with default parameters and transcript per million (TPM) were quantified by RSEM (Li  
216 and Dewey, 2011).

### 217 ***Reverse transcription PCR of D. suzukii chemosensory-related genes***

218 Expression of chemosensory receptor genes in the *D. suzukii* terminalia by RNA-seq analysis was  
219 confirmed by reverse transcription PCR (RT-PCR). *Orco* and *Gr64*, which were not found to be  
220 expressed by RNA-seq, were used as negative control and genomic DNA as positive control. The  
221 used primers are listed in Supplementary Table S2. RNA was extracted with Trizol and treated with  
222 DNase I as described before. 1  $\mu$ g RNA was then retrotranscribed to cDNA with SuperScript III  
223 Reverse Transcriptase (ThermoFisher Scientific) following the manufacturer's protocol. To control

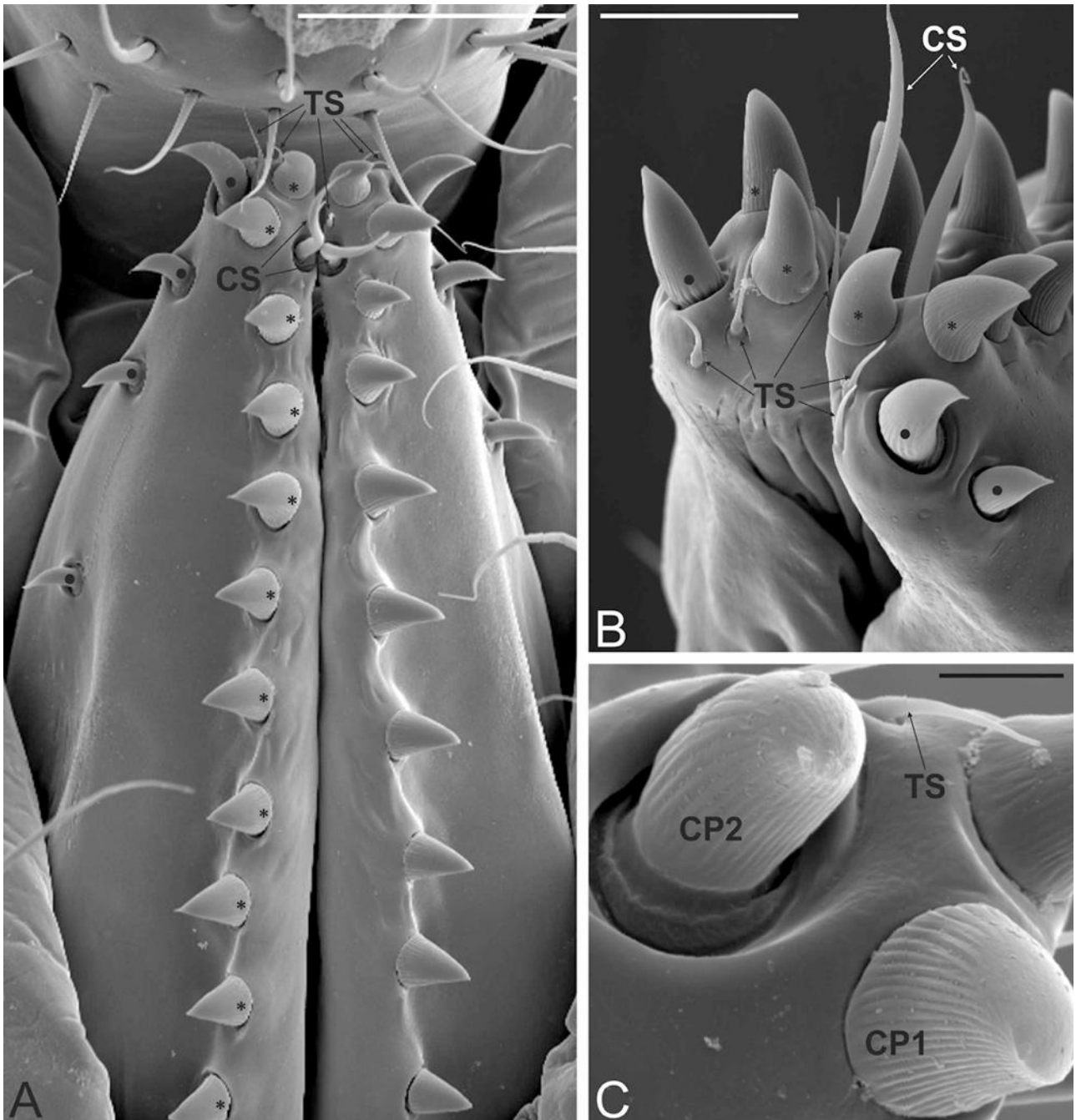
224 for genomic DNA contamination, RNA underwent a parallel mock reverse transcription step, in  
225 which the reverse transcriptase was omitted. Amplifications were carried out with GoTaq Green  
226 Master Mix (Promega) in a final volume of 25  $\mu$ l containing 1  $\mu$ l of cDNA diluted 1:10 and 0.4  $\mu$ M  
227 of each primer at the following conditions: 2 min at 95°C, then 25 cycles composed by a 30 s step at  
228 95°C, 30 s at 55°C, and 1 min at 72°C, followed by a final elongation step of 5 min at 72°C. PCR  
229 amplicons were run on 1% agarose gel stained with Midori Green Advance (Nippon Genetics).

## 230 **RESULTS AND DISCUSSIONS**

### 231 ***D. suzukii* ovipositor carries four types of mechanosensilla-like structures**

232 The ovipositor of *D. suzukii* is positioned at the very tip of the abdomen, and, at rest, is held hidden  
233 within the last abdominal segments. With a gentle pressure on the abdomen it is possible to expose  
234 the ovipositor, which comprises two elongated sub-triangular plates ending in a tip. The ovipositor  
235 of *D. suzukii*, as well as of its sister species *D. subpulchrella*, has been defined as “serrated” because  
236 of the presence of well-evident modified bristles, mostly arranged along its outer margin (*i.e.* the  
237 ventral side of the ovipositor, when considered in its resting position), giving to the ovipositor itself  
238 a jagged profile (Supplementary Figure 2) (Atallah et al., 2014). The *D. suzukii*'s ovipositor length  
239 and morphology were analysed in a comparative framework in previous studies (Atallah et al., 2014;  
240 Green et al., 2019). Of them, Atallah et al. (2014) described the external morphology and the number  
241 of bristles in *D. suzukii* and *D. subpulchrella*. Yet, ultrastructure observations or functional studies  
242 are lacking, and no information about the role these structures is known. Here, we fill the gap  
243 analysing the modified bristles present in the distal tip of the ovipositor, which are thought to come  
244 into contact with the fruit flesh (Supplementary Figure 2), whereas the more proximal unmodified  
245 bristles have not been analysed (see Atallah et al., 2014 for bristle classification). We identified four  
246 types of cuticular elements: conical pegs type 1 (CP1, also defined modified lateral bristles by Atallah  
247 et al., 2014), conical pegs type 2 (CP2, also defined modified marginal bristles by Atallah et al.,  
248 2014), and two categories of previously undescribed apical sensilla: trichoid sensilla (TS), and chaetic

249 sensilla (CS) (Figure 2, Supplementary Figure 2). The number, placement, and types of bristles on  
250 drosophilids ovipositor valves as well as the ovipositor size and shape vary greatly among species  
251 (Craddock et al., 2018). In general, all *Drosophila* species seem to have a more or less regular row of  
252 sensilla distributed on the ventral side of each valve (also called thorn bristles in *D. melanogaster*,  
253 (Chen and Baker, 1997)) and a distinctive chaetic sensilla projecting from the ventral side of the  
254 ovipositor (Craddock et al., 2018). In *D. melanogaster*, this latter is referred to as the “long bristle”  
255 (Taylor, 1989a). Other features which are not displayed by all ovipositors are dorsal or lateral sensilla  
256 and microbristles or trichoidea sensilla into the ovipositor apex (Craddock et al., 2018; Taylor,  
257 1989a).



258

259 **Figure 2. *Drosophila suzukii* ovipositor pegs and sensilla**

260 (A) Ventral view of the ovipositor of *D. suzukii* showing the two ovipositor plates and the different structures  
 261 that are present. The tip of each plate presents three trichoid sensilla (TS) and a chaetic sensillum (CS). A  
 262 single row of conical pegs type 1 (\*) is found, with the structures arranged along the ventral edge of each  
 263 ovipositor plate. Four conical pegs type 2 (●) are present, with the first one sitting at the very tip of the  
 264 ovipositor plate, while the others are positioned along a medial line of the ovipositor plate. (B) Detailed view  
 265 of the tip of the ovipositor plates. The two apical TS are clearly visible, as well as the third, inserted just behind  
 266 the most apical CP1. The CS are located very close to the TS. (C) Close-up view of the ovipositor plate tip.  
 267 The CP1 is sitting on a narrow socket; it presents a grooved cuticle that smoothens at the tip. The CP2 is sitting

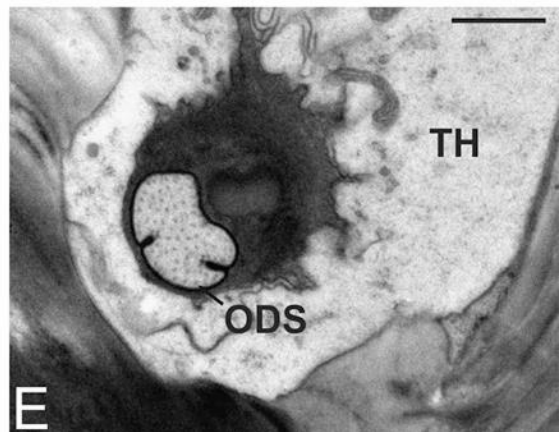
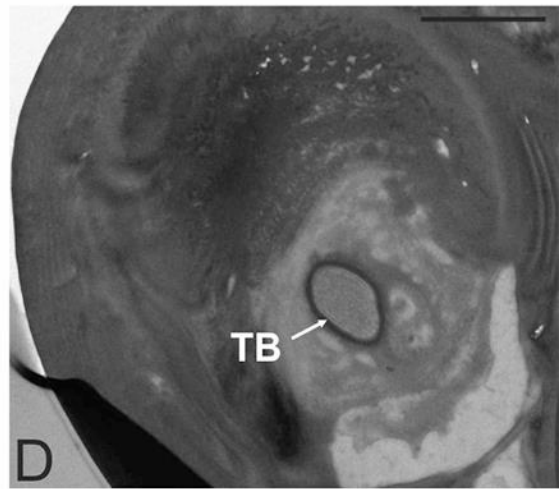
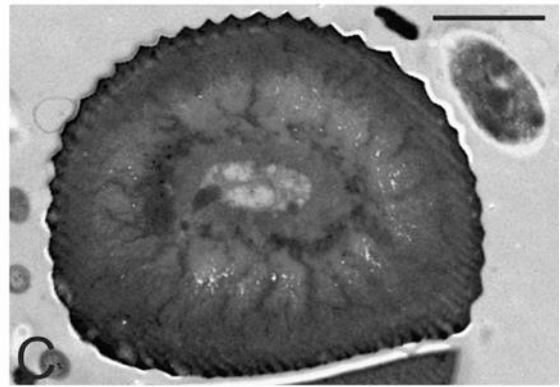
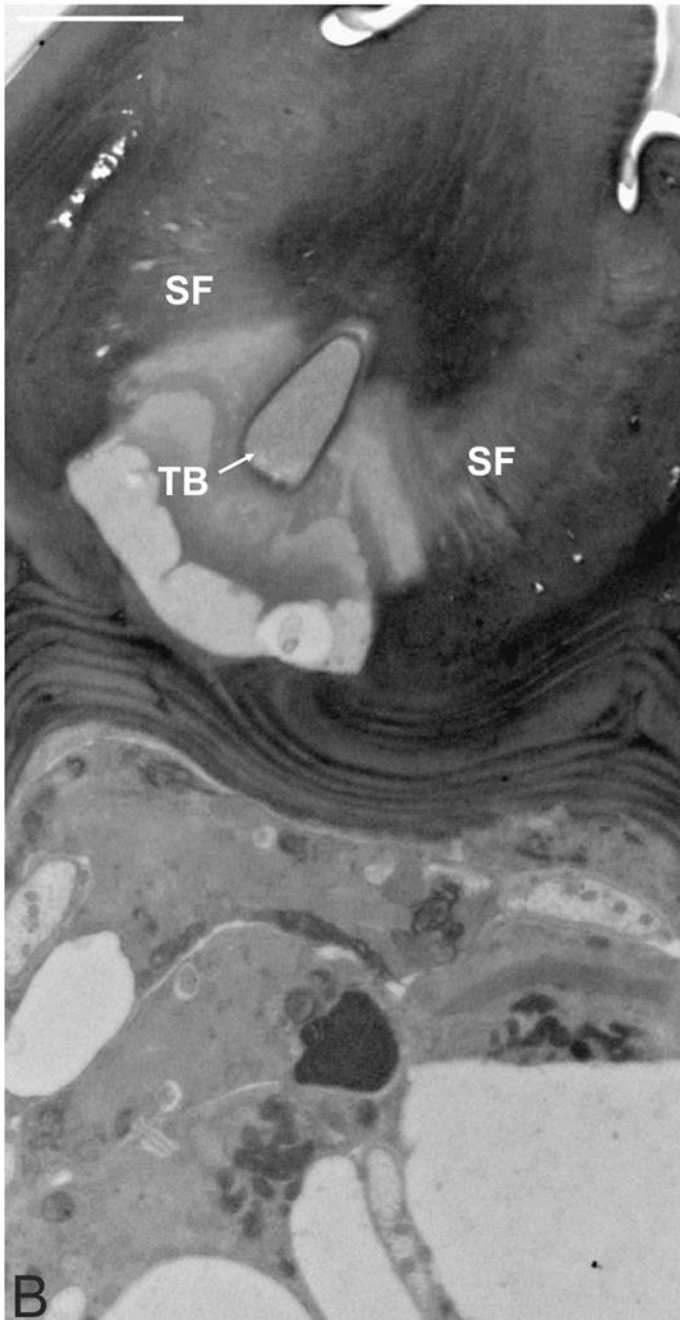
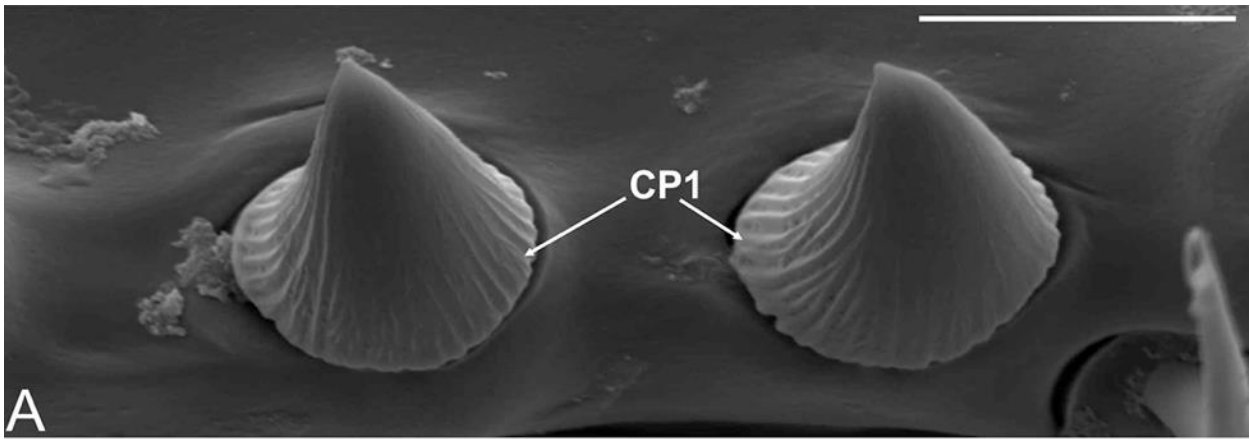
268 on a large socket; it shows a grooved cuticle as well, but with less evident grooves and a pointed tip. Scale  
269 bars: A, 50  $\mu\text{m}$ ; B, 20  $\mu\text{m}$ ; C, 5  $\mu\text{m}$ .

271 Our observations estimate an average of 17 CP1s ( $n = 50$ ,  $SD = 0.99$ ) sitting on narrow sockets  
272 in the cuticle on the ventral margin of each ovipositor plate arranged in a single row. Their number  
273 is slightly higher than what is reported by Atallah et al (2014) in two different *D. suzukii* strains,  
274 suggesting that the number of such structures may vary among individuals. Likewise, in *D.*  
275 *melanogaster*, the observed number of thorn bristles (the structures homologous to CP1s) varies from  
276 11 to 17 (Chen and Baker, 1997; Taylor, 1989a). CP1 number did not differ significantly between *D.*  
277 *suzukii* and *D. subpulchrella* (Atallah et al., 2014). Our observations revealed that CP1s are about 15  
278  $\mu\text{m}$  long with a base diameter of 10  $\mu\text{m}$  and are characterised by a cuticular shaft slightly bent towards  
279 the external side of the plate (Figure 2A). The cuticle is grooved externally all along (Figure 3A).  
280 Each structure ends in a sharp tip, although in some specimens the tip appears worn, having a blunt  
281 shape. The analysis of ultrathin sections shows that the internal structure is characterised by a solid,  
282 poreless cuticular shaft (Figure 3B). Micrographs taken at the level of the medial peg show a thick  
283 and continuous cuticular wall with a small lumen without sensory neurons (Figure 3C). Imaging at  
284 the socket level shows the presence of a single sensory neuron embedded in an electron-dense  
285 dendrite sheath, and ending in a tubular body (Figure 3D and E). The tubular body is located at the  
286 base of the peg, where the socket with suspension fibres is evident (Figure 3B). In insects, the tubular  
287 body is a cellular feature of mechanoreceptors since it is required for mechanotransduction and its  
288 absence causes a loss of mechanosensitivity (Erler, 1983; Keil and Steinbrecht, 1984; Marshall and  
289 Lumpkin, 2012). In *D. melanogaster* the tubular body is typical of type I sensory neurons that  
290 construct cilia or flagella, which include bristle mechanoreceptors and proprioceptors such as  
291 chordotonal organs and campaniform sensilla (Gillespie and Walker, 2009; Kernan, 2007). All these  
292 evidences strongly suggest that CP1s are mechanosensilla.

293 In *D. melanogaster*, the anti-HRP staining of the ventral thorn bristles corresponding to *D.*  
294 *suzukii* CP1s provided evidences of their sensory nature (Taylor, 1989a, 1989b). Labelling of *D.*  
295 *suzukii* ovipositor tip with anti-HRP is consistent with ultrastructure observations and shows the  
296 presence of a single sensory neuron that terminates at the base of each CP1 (Figure 4). *D.*  
297 *melanogaster* thorn bristles were labelled with the pan-neuronal marker *n-syb* revealing the presence  
298 of a single neuron ending at the base of each bristle, likewise to the anti-HRP staining in *D. suzukii*  
299 (Figure 4). This anatomical similarity between *D. suzukii* and *D. melanogaster* suggests that also in  
300 the latter species, ventral ovipositor bristles could be mechanosensitive structures. Hence, CP1  
301 function could be conserved in the ovipositor of *Drosophila* species independently of the ovipositor  
302 shape. This is consistent with results from Craddock et al. (2018) that did not identify any pore on  
303 the surface of ventral bristles in 41 Hawaiian drosophilids with dramatic differences in ovipositor  
304 morphology. However, further functional and structural studies are needed to rigorously falsify this  
305 hypothesis in *D. melanogaster* and other *Drosophila* species.

306

307



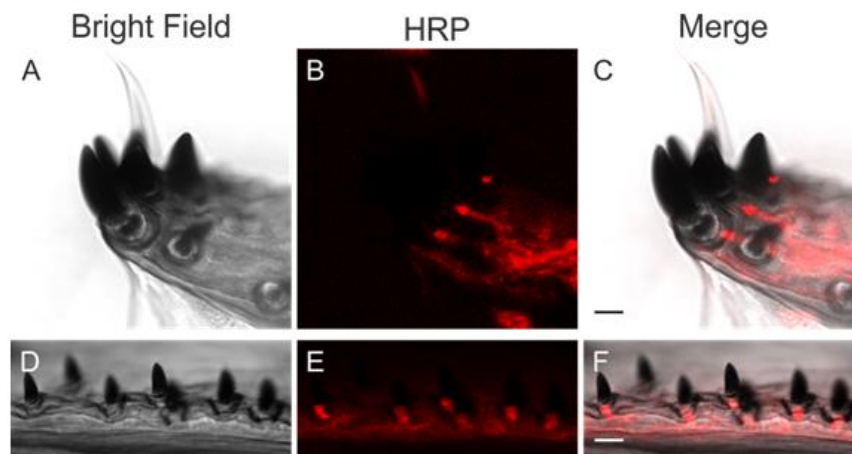
308  
309  
310

Figure 3. Micrographs showing details of the conical pegs type 1 of the *Drosophila suzukii* ovipositor.

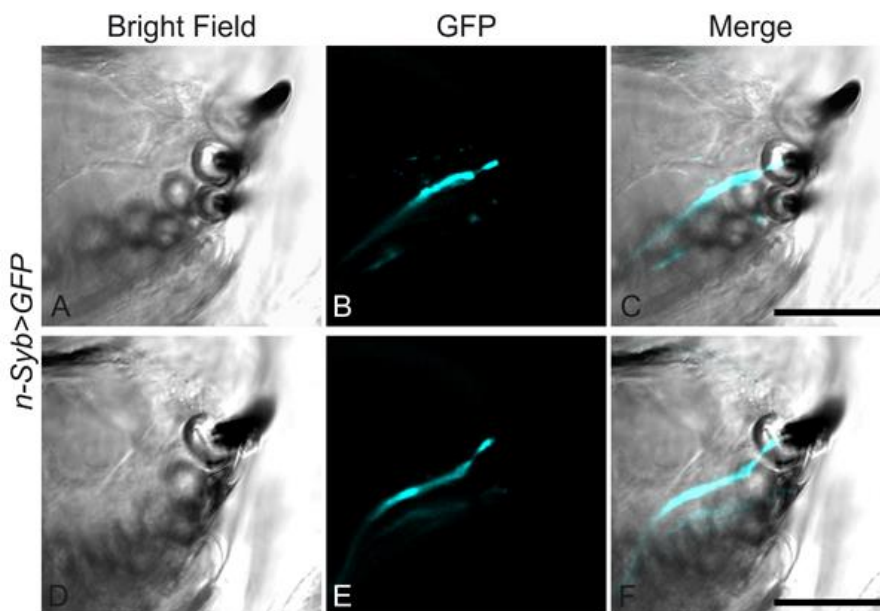


311 (A) Scanning electron microscopy (SEM) ventral view of parts of the ovipositor plate ridge showing two  
 312 conical pegs type 1 (CP1). (B) Transmission electron microscopy (TEM) longitudinal section at the socket  
 313 level. The peg is sitting on a narrow socket made of thick cuticle. Suspension fibres (SF) are apparent, holding  
 314 the peg and giving flexibility to the structure. The single sensory neuron associated with the CP1 terminates  
 315 in a tubular body (TB) ending just at the base of the peg. (C-E) Serial TEM micrographs of a CP1 cross  
 316 sections, taken at different levels, show the solid cuticular structure of the peg (C), the presence of the tubular  
 317 body (TB) at the socket level (D), and the outer dendritic segment (ODS) of the sensory neuron enclosed by  
 318 the thecogen cell (TH) (E). Scale bars: A, 10  $\mu\text{m}$ ; B-D, 2  $\mu\text{m}$ ; E, 1  $\mu\text{m}$ .

*Drosophila suzukii*



*Drosophila melanogaster*



319  
 320 **Figure 4. Conical pegs are innervated by single neurons in both *Drosophila suzukii* and *D. melanogaster***  
 321 **ovipositors.**

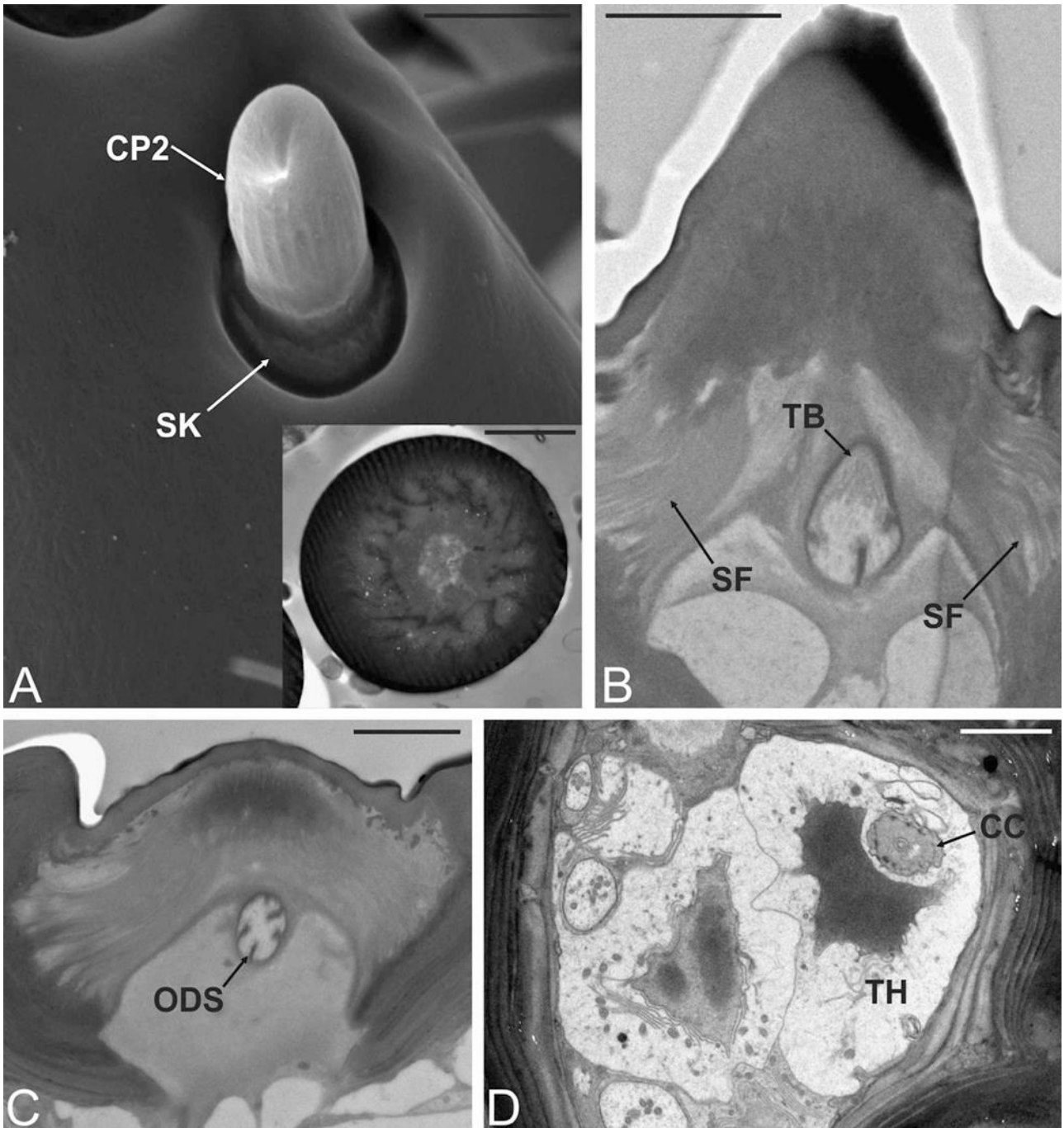
322 Upper panel: Immunostaining of cryosection of the *D. suzukii* ovipositor plate: (A and D) bright-field, (B and  
 323 E) counter staining with anti-horseradish peroxidase (HRP) to visualize the neuron, (C and F) merged pictures.

324 Scale bars: 10  $\mu\text{m}$ . Lower panel: The pan-neuronal marker *n-syb* showed a single neuron innervating all  
325 ovipositor pegs in *D. melanogaster*. (**A and D**) bright-field, (**B and E**) green fluorescent protein (GFP)  
326 visualization, (**C and F**) merged pictures. Scale bars: 20  $\mu\text{m}$ .

327

328 Our observations reveal four to five CP2s arranged in line starting from the tip of each  
329 ovipositor plate (Figure 2A). They are smaller than CP1s and show decreasing sizes from the most  
330 apical (14.5  $\mu\text{m}$  long and 6  $\mu\text{m}$  of base diameter) to the proximal one (12.5  $\mu\text{m}$  long and 3.5  $\mu\text{m}$  of  
331 base diameter). Atallah et al. (2014) reported that size differences between CP1s and CP2s are less  
332 pronounced in *D. subpulchrella* than in *D. suzukii*, while in *D. melanogaster* no bristles equivalent to  
333 CP2s have been found (Taylor, 1989a). The cuticular shaft of CP2 is slightly grooved along the  
334 longitudinal axis for most of its length, although grooves are not as evident as in CP1 (Figure 2C).  
335 Each CP2 ends in a fine tip that is absent in case of mechanical abrasion. The peg is sitting on an  
336 evident socket within the cuticular wall of the plate (Figure 5A). TEM investigation revealed an  
337 internal structure similar to CP1, *i.e.* the presence of a solid cuticular shaft, devoid of pores (see inset  
338 in Figure 5A), a small internal lumen without sensory neurons, and a single sensory neuron with a  
339 distal tubular body attached at the base of the peg (Figure 5B-D). The peg itself is attached flexibly  
340 to the cuticle through a large socket with an abundance of suspension fibres (Figure 5B). Anti-HRP  
341 staining highlights the presence of a single sensory neuron that stops at the base of each CP2 (Figure  
342 4). All these evidences suggest that CP2s are mechanosensitive structures likewise CP1s.

343

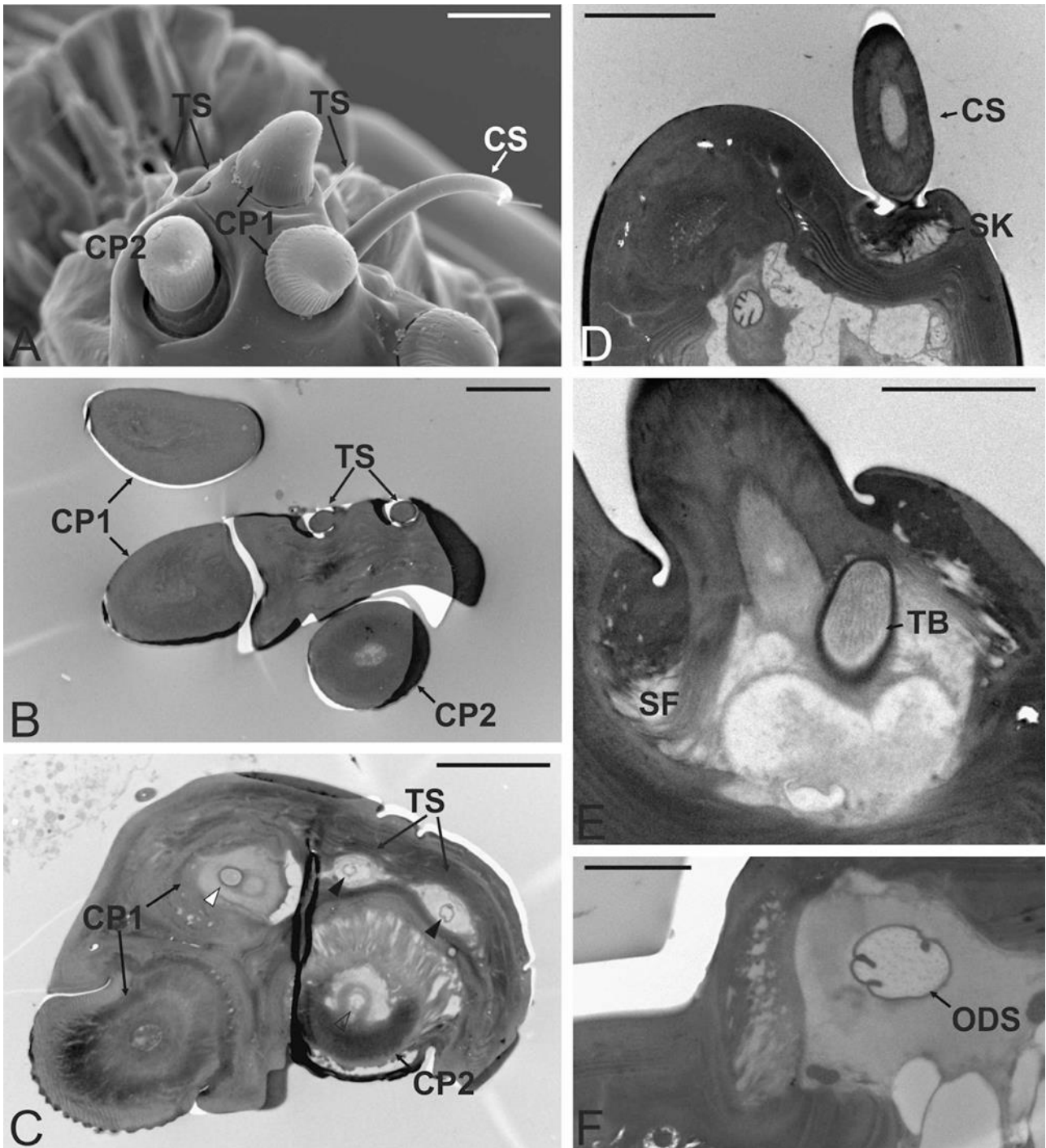


344  
 345 **Figure 5. Micrographs showing details of the conical pegs type 1 of the *Drosophila suzukii* ovipositor (A)**  
 346 SEM ventral view of the ovipositor plate, showing one of the conical pegs type 2 (CP2), with a slightly grooved  
 347 cuticle and a sharp tip. Noticeable is also the large socket (SK) on which the CP2 is sitting in the cuticular wall  
 348 of the ovipositor plate. The inset in (A) shows the TEM micrograph of a CP2 cross section, taken at half of the  
 349 length of the peg: the peg is made of solid, thick cuticle, and presents a reduced lumen, devoid of sensory  
 350 neurons. (B-D) Serial TEM micrographs of a CP2, longitudinally and cross sections taken at different levels.  
 351 They show in (B) the base of a CP2 with a large flexible socket and several suspension fibres (SF). The single  
 352 sensory neuron ends in a tubular body (TB) at the base of the peg. In (C) the large socket is visible, as well as  
 353 the outer dendritic segment (ODS) of the sensory neuron. In (D) a cross section is imaged at a lower level

354 respect to the previous: the sensory neuron appears at the ciliary constriction level (CC), and it is enclosed by  
355 the thecogen cell (TH). Scale bars: A, 5  $\mu\text{m}$ ; inset in A, 2  $\mu\text{m}$ ; B-D, 2  $\mu\text{m}$ .

356  
357 At the apex of each *D. suzukii* ovipositor plate, there are three small TS (Figure 2B). Two are  
358 located on the dorsal side of the plate, whereas the third one is located apically (Figure 6A). In *D.*  
359 *melanogaster*, three trichoid ovisensilla have also been reported (Taylor, 1989a). In *D. suzukii*, they  
360 are slender and finely tipped sensilla with a smooth cuticular shaft devoid of cuticular pores (12.5  $\mu\text{m}$   
361 long and 1.5  $\mu\text{m}$  of base diameter). These sensilla are sitting in the cuticular wall on distinct sockets,  
362 running almost parallel to the plate cuticular wall itself. TEM images reveal that TS are made of solid  
363 cuticle, there are no pores on the cuticle and no sensory neurons entering the peg lumen (Figure 6B).  
364 A single sensory neuron is associated with each TS, reaching the sensillum base through a distal  
365 tubular body (Figure 6C and Supplementary Figure S3). In *D. melanogaster*, these three trichoidea  
366 sensilla appeared innervated by multiple neurons and have been hypothesized to be endowed with  
367 chemosensory functions (Taylor, 1989b). However, our observations in *D. suzukii* clearly discard a  
368 role in chemosensation.

369 Each ovipositor plate shows the presence of a single CS inserted into the inner face of each  
370 valve tip. It is long (38  $\mu\text{m}$ ) and slender (2.5  $\mu\text{m}$  of base diameter), with a typical curved shape and a  
371 very fine tip (Figure 6A). It is sitting on a large socket in the plate wall. Externally, the CS wall is  
372 smooth. Serial ultrathin sections revealed that the CS cuticular shaft is made of solid cuticle and  
373 shows a central lumen without neurons (Figure 6D). At the base, the shaft is attached to the cuticle  
374 and suspended through an elaborated socket with numerous suspension fibres (Figure 6E). A single  
375 sensory neuron ends in a tubular body that attaches at the sensillum base (Figure 6F). This is a typical  
376 feature of mechanosensitive-like organs, and together with the absence of pores on the surface of the  
377 *D. suzukii* CS clearly points out a likely function in mechanotransduction. However, in two groups  
378 of Hawaiian *Drosophila* species, the apical CS (referred to as “long subapical sensillum”) is  
379 uniporous, thus suggesting that in some species it may have taste function that helps to exploit specific  
380 ecological microniches (Craddock et al., 2018).



382

383

**Figure 6. Micrographs showing details of the trichoid sensilla and chaetic sensilla.**

384

(A) Scanning electron microscopy (SEM) picture of the ovipositor plate tip showing the three trichoid sensilla

385

(TS) and the single chaetic sensilla (CS). (B-C) Serial transmission electron microscopy (TEM) cross sections

386

of the ovipositor plate. In (B) the section is taken most apically and shows the two TS made of solid cuticles

387

entering the cuticular wall, no sensory neurons were detected at this level. In (C) the two TS are pictured more

388

proximally, the peg is no longer visible but two sensory neurons (one per each TS) are visible (black

389

arrowheads). White and blank arrowheads show the sensory neurons associated with conical pegs type 1 (CP1)

390 and type 2 (CP2), respectively. **(D-F)** Serial TEM longitudinal sections showing the main ultrastructural  
391 features of a CS: in **(D)** the CS is taken at the socket level (SK) and shows a thick cuticle with a central lumen  
392 without sensory neurons; in **(E)** a single sensory neuron ending in a tubular body (TB) inserted at the CS base  
393 is visible. The socket presents numerous suspension fibres (SF). In **(F)** the outer dendritic segment (ODS) of  
394 the sensory neuron is visible. Scale bars: A, 10  $\mu\text{m}$ ; B-C-D, 5  $\mu\text{m}$ ; E-F, 2  $\mu\text{m}$ .

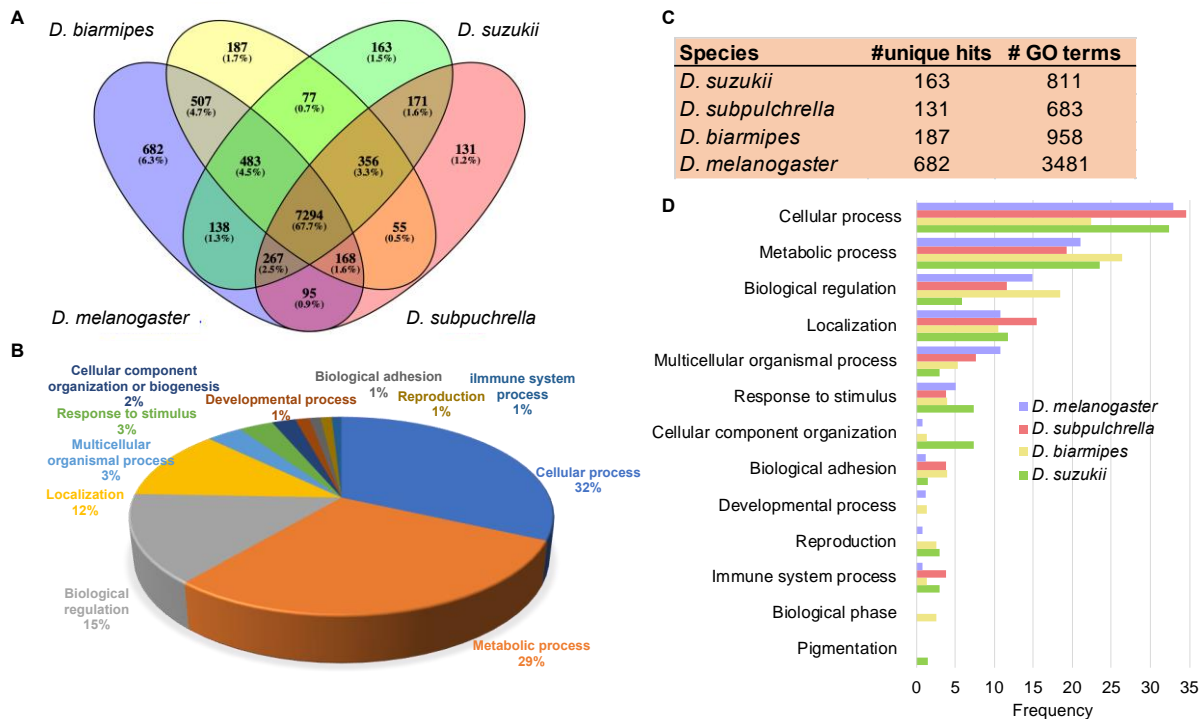
395

### 396 ***RNA-seq characterization of the terminalia of four Drosophila species***

397 Since variation in egg-laying sites and ovipositor morphology among *Drosophila* species exists, we  
398 were interested in determining whether there is a corresponding level of variation in gene-expression  
399 comparing *de novo* assembled transcriptomes from the terminalia of four *Drosophila* species with  
400 different ovipositor shapes and egg-laying behaviors (Figure 1). Female terminalia can be divided in  
401 two parts, genitalia and analia. The genitalia comprise the external ovipositor plates and the internal  
402 ducts of the reproductive system, whereas the analia are made by the external anal plates and the  
403 posterior hindgut (Taylor, 1989a). Thus, our RNA-seq analysis reflects transcripts expressed in all of  
404 these tissues.

405 Illumina RNA-seq libraries from the terminalia of four *Drosophila* species generated an  
406 average of 60M ( $\pm 2.4\text{M}$  SD) 100 bp paired-end reads that led to four *de novo* assembled  
407 transcriptomes with contig counts ranging from 31,315 (*D. subpulchrella*) to 40,162 (*D. suzukii*)  
408 (Supplementary Table S1). Although reference genomes for three out of four *Drosophila* species  
409 studied were available, in the present study, transcripts were *de novo* assembled instead of mapping  
410 to genomic sequences because of the dramatic differences in genome completeness and resolution  
411 that would affect the detection of several transcripts. Our strategy has yielded four assemblies of  
412 comparable number of contigs ( $34884 \pm 4017$ ), N50 ( $2728 \pm 4588$ ) and percentage of reads  
413 successfully aligned to the assemblies ( $80 \pm 6$ ) (Supplementary Table S1). Thus, they are appropriate  
414 for a comparative analysis aimed to study transcript composition among assemblies, and presence or  
415 absence of specific transcripts. We used blastx to identify homologous genes in *D. melanogaster* and  
416 assign gene ontology (GO) terms to our contigs. On average, 70% of contigs from each of the four

417 transcriptomes has a blastx hit against the *D. melanogaster* predicted proteome (Supplementary  
418 Dataset S1). Unique hits retrieved for each species vary from 8,537 (*D. subpulchrella*) to 9,634 (*D.*  
419 *melanogaster*). Of these, 7,294 hits are common among the four *Drosophila* species, and represent  
420 the conserved transcriptional core for the *Drosophila* terminalia (Figure 7A). GO analysis shows that  
421 the common terminalia genes are mostly involved in cellular processes (32%), metabolic processes  
422 (29%), and biological regulation (15%) (Figure 7B). Species-specific hits are few, namely 163 for *D.*  
423 *suzukii*, 131 for *D. subpulchrella*, 187 for *D. biarmipes*, and 682 for *D. melanogaster*, respectively.  
424 Unique *D. suzukii* hits have 811 unique GO terms (Figure 7C, and Supplementary Dataset S2).  
425 Among them there are contigs homologous to genes involved in pigmentation, cellular component  
426 organization, and response to stimulus compared to the other species (Figure 7D). Contigs annotated  
427 with pigmentation are homologous to *yellow-g2*. Proteins belonging to yellow gene family are  
428 involved in the synthesis of melanic pigment (Ferguson et al., 2011; Gompel et al., 2005), which may  
429 be related to the phenotypic plasticity of *D. suzukii*, whose winter morph phenotype is characterized  
430 by darker pigmentation (Shearer et al., 2016). Contigs annotated to cellular component organization  
431 are homologous to genes related to ribosome biogenesis. The ovipositor of *D. suzukii* has bigger  
432 ovipositor cells than *D. melanogaster* (Green et al., 2019), and this expression of contigs related to  
433 ribosome biogenesis may reflect the cost of cell maintenance.



434

435 **Figure 7. Annotation of transcriptomes from the terminalia of four *Drosophila* species.**

436 (A) Venn diagram representing the unique *D. melanogaster* gene hits retrieved by blastx searches using contigs  
 437 from each assembly as query. (B) Gene Ontology (GO) classification for the 7294 gene hits common to the  
 438 four assemblies referred to Biological Process (Panther GO-Slim terms). (C) Number of species-specific hits  
 439 and associated GO terms (D) GO classification for species-specific hits referred to biological processes  
 440 (Panther GO-Slim terms). Abbreviations: Dmel, *D. melanogaster*; Dbia, *D. biarmipes*; Dsuz, *D. suzukii*;  
 441 Dsubp, *D. subpulchrella*.

442 ***Conserved set of transcripts associated with mechanotransduction in Drosophila terminalia***

443 Given the ultrastructure analysis revealed that *D. suzukii* ovipositor pegs and sensilla are  
 444 mechanosensitive-like structures, we were interested in determining which mechanosensitive  
 445 channels and other sensory-related transcripts are expressed in terminalia. Our data allow us to  
 446 explore in detail the presence-absence of transcripts in the different species. We specifically looked  
 447 for contigs orthologous to mechanosensitive genes described so far in *D. melanogaster* (Karkali and  
 448 Martin-Blanco, 2017): the putative metazoan mechanotransduction channels, *i.e.* degenerin/epithelial  
 449 Na<sup>+</sup> channel C (DeG/eNaC) (Adams et al., 1998; Gorczyca et al., 2014; Guo et al., 2014; Jang et al.,  
 450 2019; Tsubouchi et al., 2012; Zhong et al., 2010), the transient receptor potential (TRP) channels  
 451 (Cheng et al., 2010; Gong et al., 2004; Göpfert et al., 2006; Tracey et al., 2003; Tsubouchi et al.,



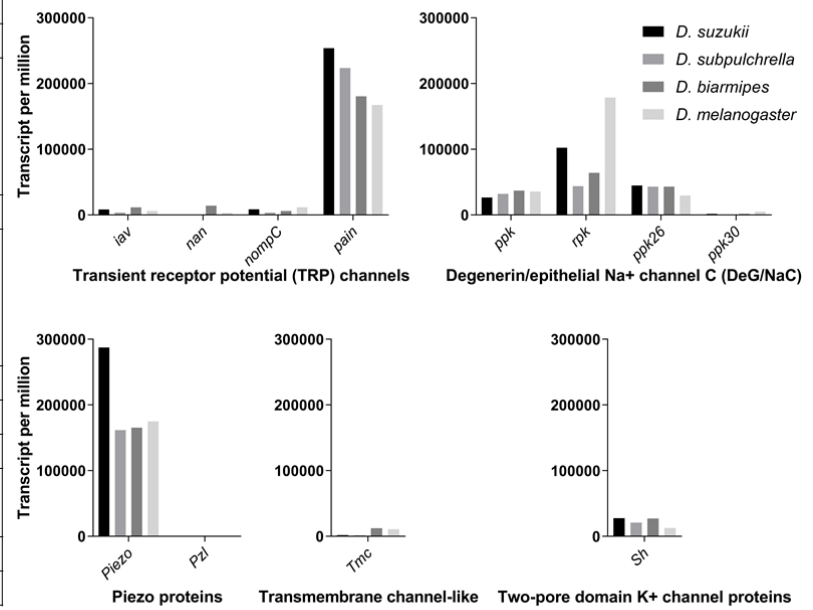
452 2012; Walker et al., 2000), the two-pore domain K<sup>+</sup> channel proteins (K2P) (Tabarean and Morris,  
453 2002), as well as *piezo* (Kim et al., 2012), *piezo-like* (*pzl*) (Hu et al., 2019) and *transmembrane*  
454 *channel-like* (*tmc*) genes (Guo et al., 2016).

455 Consistent with the results of the ultrastructural analysis, a conspicuous number of  
456 mechanosensitive-related transcripts are present in the *D. suzukii* assembly (Figure 8). However, all  
457 the candidate mechanosensitive genes present in *D. suzukii* terminalia transcriptome are commonly  
458 present in more than one of the other *Drosophila* assemblies (Table 1), pointing out that  
459 mechanosensation is a feature equally present in the terminalia of all species. Among genes whose  
460 expression is completely shared among the four species there are three DeG/eNaC proteins (which in  
461 *Drosophila* are commonly referred to as pickpocket proteins): *ppk*, *rpk*, and *ppk26* (Adams et al.,  
462 1998; Gorczyca et al., 2014; Tsubouchi et al., 2012; Zhong et al., 2010). Only transcripts encoding a  
463 fourth pickpocket protein (*ppk30*), which has been recently related to mechanotransduction in *D.*  
464 *melanogaster* (Jang et al., 2019), are absent in all samples. Also *piezo*, its paralog *pzl*, as well as  
465 *shaker* and *painless* (*pain*) have a presence-absence pattern conserved across species. The four  
466 assemblies contain contigs homologous to *piezo*, that is a transmembrane protein involved in  
467 mechanosensitive nociception in *D. melanogaster* (Kim et al., 2012), but not to *pzl*. Contigs  
468 homologous to *shaker*, which is a K2P stretch-sensitive ion channel (Tabarean and Morris, 2002), are  
469 present in the four assemblies as well as contigs homologous to *pain*, which codes for a TRP channel  
470 required for both thermal and mechanical nociception (Tracey et al., 2003).

471 In a subset of assemblies, we could detect transcripts of *tmc* and TRP channels other than *pain*  
472 involved in mechanotransduction. *tmc* is expressed in *D. melanogaster* larval peripheral sensory  
473 neurons, and it is involved in proprioception and sensory control of larval locomotion (Guo et al.,  
474 2016). Contigs homologs to this gene were found only in *D. melanogaster* and *D. biarmipes*  
475 assemblies, while they were absent in transcriptomes from species with serrated ovipositors. TRP  
476 proteins are membrane proteins that mediate many forms of sensory perception, including  
477 mechanosensation. Among TRPs involved in mechanotransduction, *no mechanoreceptor potential C*

478 (*nompC*), which is the *bona fide* mechanotransduction channel in *Drosophila* (Walker et al., 2000) is  
479 present only in *D. suzukii* and *D. melanogaster* assemblies. Contigs homologous to *inactive* (*iav*) are  
480 absent in *D. subpulchrella* assembly, and contigs homologous to *nanchung* (*nan*) are present only in  
481 the *D. biarmipes* assembly. Since *iav* and *nan* encode interdependent channel subunits and require  
482 each other for expression in *D. melanogaster* (Gong et al., 2004), we sought to understand why we  
483 found transcripts corresponding to only one of the two transcripts in the assemblies of *D. suzukii* and  
484 *D. melanogaster*. One reason might be due to their specific expression in few cells that has been  
485 diluted by the sequencing of a composite tissue such as the terminalia (Johnson et al., 2013). To  
486 explore if the absence of some transcripts is due to artifacts, we quantified expression of manually  
487 annotated mechanosensitive-related genes in each species (Figure 8, Supplementary Dataset S3).  
488 Although the absence of replicates does not allow us to study in depth species-specific expression  
489 patterns, expression levels may indicate if a specific gene has similar mRNA levels among the four  
490 species. Our data reveal that all genes showing an inconsistent presence-absence pattern across  
491 species (*iav*, *nan*, *nompC* and *tmc*) have a low expression signal in all *Drosophilas*. Thus, their  
492 absence from some *de novo* assembled transcriptome may be due to limiting number of reads  
493 available for assembling. Interestingly, likewise genes with an inconsistent presence-absence pattern,  
494 also genes present in the four assemblies have similar mRNA levels across species.

Gene symbol	<i>D. suzukii</i> assembly	Other <i>Drosophila</i> assemblies
<b>Degenerin/epithelial Na<sup>+</sup> channel C (DeG/eNaC)</b>		
<i>ppk</i>	Present	Present
<i>rpk</i>	Present	Present
<i>ppk26</i>	Present	Present
<i>ppk30</i>	Absent	Absent
<b>Transient receptor potential (TRP) channels</b>		
<i>pain</i>	Present	Present
<i>nompC</i>	Present	<i>D. melanogaster</i>
<i>iav</i>	Present	<i>D. biarmipes</i> , <i>D. melanogaster</i>
<i>nan</i>	Absent	<i>D. biarmipes</i>
<b>Two-pore domain K<sup>+</sup> channel proteins (K2P)</b>		
<i>Sh</i>	Present	Present
<b>Piezo proteins</b>		
<i>Piezo</i>	Present	Present
<i>Pzl</i>	Absent	Absent
<b>Transmembrane channel-like (TMC) proteins</b>		
<i>Tmc</i>	Absent	<i>D. biarmipes</i> , <i>D. melanogaster</i>



495

496 **Figure 8. Annotation of transcriptomes from the terminalia of four *Drosophila* species.**

497 **(Left panel)** Table highlighting the presence or absence of contigs orthologous to *Drosophila melanogaster*  
498 mechanosensitive genes in *D. suzukii de novo* transcriptome assembly and in the other three assemblies. **(Right**  
499 **panel)** Quantification of mRNA levels of mechanosensitive genes in *D. melanogaster*, *D. suzukii*, *D. biarmipes*  
500 and *D. subpulchrella* terminalia. Trimmed reads were mapped against manually annotated mechanosensitive  
501 genes except for *D. subpulchrella*, whose reads were mapped against the sister-species *D. suzukii* annotation  
502 set.

### 503 *Expression of chemosensory-related genes in terminalia*

504 The four assemblies contain contigs homologous to genes involved in chemosensory perception, *i.e.*  
505 several gustatory receptors (GRs), ionotropic receptors (IRs), and odorant receptors (ORs)  
506 (Supplementary Table 3). In particular, contigs homologous to *Ir47a* are present in all four  
507 assemblies, and contigs homologous to *Ir62a* and *Gr66a* are present in three out of four assemblies.  
508 Interestingly, these three genes are among the most expressed ones in all species (Supplementary  
509 Figure S4). Among the other highest expressed chemoreceptor genes there is *Or43b*. Surprisingly,  
510 we did not find any trace of the olfactory receptor co-receptor (*Orco*) expression, which is required  
511 to have functional odorant receptors (Joseph and Carlson, 2015). In *D. suzukii*, *Orco* absence has  
512 been confirmed by RT-PCR (Supplementary Figure S5).

513 The genomes of *D. suzukii* or *D. biarmipes* contain several paralogous genes that encode  
514 chemoreceptor and are not shared with *D. melanogaster* (Crava et al., 2016; Ramasamy et al., 2016).  
515 Gene duplication may be source of novel properties, *e.g.* paralogs may be expressed in body parts  
516 other than the ancestral expression site where they take care of new functions (Kaessmann, 2010).  
517 No paralogous genes are present in *D. suzukii* and *D. biarmipes* terminalia transcriptomes, pointing  
518 out that duplicated chemoreceptor genes identified in these species do not carry out any new function  
519 in this appendage.

520 Expression of chemoreceptor genes in *D. suzukii* terminalia should not be related to the  
521 presence of sensilla and pegs on the tip of the ovipositor valves, since ultrastructure analysis detailed  
522 features compatible only with mechanosensitive-like organs. However, chemosensory structures may  
523 be present in other tissues in the terminalia, such as the analia (Supplementary Figure S1). In *D.*  
524 *melanogaster*, analia carry several small and long bristles. In addition, the eighth tergite, which wraps  
525 the anal plate, is scattered with thin bristles (Taylor, 1989a). Moreover, it has been shown that, besides  
526 the main function in taste, some GRs (and likely some IRs) may have other non-gustatory functions,  
527 such as the detection of internal ligands. For example, internal sensory neurons are present in the  
528 reproductive tract of *D. melanogaster* to sense sex peptide (Lee et al., 2016; Naccarati et al., 2012),  
529 and this may be a location, where chemoreceptor transcripts are expressed. *Gr43a*, which is involved  
530 in fructose detection in the *D. melanogaster* brain, is also expressed in the female uterus, possibly for  
531 the detection of fructose in the seminal fluid (Sato et al., 2011). *Gr43a* was found only in *D. biarmipes*  
532 assembly, and its expression levels in the four species are quite low, possibly due to an expression  
533 pattern limited to few cells. The other taste receptors present in the assemblies may have similar  
534 physiological roles in internal sensing.

535

## 536 CONCLUSIONS

537 Our results represent the first step towards a full molecular, anatomical, and physiological  
538 characterization of sensory perception in the ovipositor of *D. suzukii*. In particular, these findings (i)

539 show that pegs and sensilla housed in the tip of the *D. suzukii* ovipositor have a mechanosensilla-like  
540 structure, (ii) indicate that such feature may be shared with *D. melanogaster*, another species with  
541 blunt-end ovipositor, (iii) provide a qualitative overview of genes expressed in the terminalia of four  
542 *Drosophila* species with different ovipositor shapes. We propose that the sensilla and pegs present  
543 on the ovipositor tip of *D. suzukii* are the sensory structures responsible to probe substrate stiffness  
544 for the egg-laying site selection. It is also possible that these sensory structures work together with  
545 other sensory organs in assessing when the ovipositor has penetrated the substrate and peristaltic  
546 waves can start pushing down the egg. Previous research has demonstrated that fruit stiffness is the  
547 crucial component in host selection and is negatively related to oviposition and, as a consequence,  
548 fruit susceptibility to *D. suzukii* (Baser et al., 2018; Ioriatti et al., 2015; Kinjo et al., 2013; Lee et al.,  
549 2011). In this wider context, our work provides a necessary starting point to elucidate the molecular  
550 and physiological basis of the mechanotransduction system in the ovipositor of *D. suzukii*, which  
551 might allow for the development of mechanotransduction-based control strategies. Furthermore, we  
552 suggest that ovipositor mechanosensitive-like organs are likely to be of evolutionary importance  
553 across *Drosophila* species independently of the ovipositor shape. Future functional studies will clarify  
554 the relationship between the structure and the function of the ovipositor sensilla.

555

556

## 557 **AUTHOR CONTRIBUTIONS**

558 CMC participated in the design of the study, carried out the RNA-seq analysis, participated in the  
559 neuronal staining experiments, and drafted the manuscript; RR participated in the design of the study,  
560 carried out the ultraimaging experiments and critically revised the manuscript; DZ participated in the  
561 design of the study, participated in the neuronal staining experiments, carried out the visualization of  
562 the GFP expression, and critically revised the manuscript; SA carried out the molecular work, and  
563 participated in the neuronal staining experiments and the visualization of GFP expression; GS, RC,  
564 AH, MP, VRS, ORS, and GT participated in the design of the study and critically revised the

565 manuscript, GA conceived of the study, designed the study, coordinated the study, and critically  
566 revised the manuscript.

567

## 568 **FUNDING**

569 Cristina M. Crava has been a recipient of a FP7-PEOPLE- 2013-IEF grant from the European Union  
570 (grant ID 627755). This research was funded by the Italian Ministry of Education, University and  
571 Research (program MIUR-FFABR 2017) to Albrecht Haase.

572

## 573 **BIBLIOGRAPHY**

574 Adams, C., Anderson, M.G., Motto, D., Price, M., Johnson, W.A., Welsh, M.J., 1998. Ripped  
575 pocket and pickpocket, novel *Drosophila* DEG/ENaC subunits expressed in early development  
576 and in mechanosensory neurons. *J. Cell Biol.* 140, 143–152.

577 Aranha, M.M., Vasconcelos, M.L., 2018. Deciphering *Drosophila* female innate behaviors. *Curr.*  
578 *Opin. Neurobiol.* 52, 139–148. <https://doi.org/10.1016/j.conb.2018.06.005>

579 Asplen, M.K., Anfora, G., Biondi, A., Choi, D.S., Chu, D., Daane, K.M., Gibert, P., Gutierrez,  
580 A.P., Hoelmer, K.A., Hutchison, W.D., Isaacs, R., Jiang, Z.L., Kárpáti, Z., Kimura, M.T.,  
581 Pascual, M., Philips, C.R., Plantamp, C., Ponti, L., Vétek, G., Vogt, H., Walton, V.M., Yu, Y.,  
582 Zappalà, L., Desneux, N., 2015. Invasion biology of spotted wing *Drosophila* (*Drosophila*  
583 *suzukii*): a global perspective and future priorities. *J. Pest Sci.* (2004).

584 <https://doi.org/10.1007/s10340-015-0681-z>

585 Atallah, J., Teixeira, L., Salazar, R., Zaragoza, G., Kopp, A., 2014. The making of a pest: the  
586 evolution of a fruit-penetrating ovipositor in *Drosophila suzukii* and related species. *Proc. R.*  
587 *Soc. B Biol. Sci.* 281, 20132840. <https://doi.org/10.1098/rspb.2013.2840>

588 Baser, N., Broutou, O., Verrastro, V., Porcelli, F., Ioriatti, C., Anfora, G., Mazzoni, V., Rossi  
589 Stacconi, M. V., 2018. Susceptibility of table grape varieties grown in south-eastern Italy to  
590 *Drosophila suzukii*. *J. Appl. Entomol.* 142, 465–472. <https://doi.org/10.1111/jen.12490>

- 591 Bolger, A.M., Lohse, M., Usadel, B., 2014. Trimmomatic: A flexible trimmer for Illumina sequence  
592 data. *Bioinformatics* 30, 2114–2120. <https://doi.org/10.1093/bioinformatics/btu170>
- 593 Chen, E.H., Baker, B.S., 1997. Compartmental organization of the *Drosophila* genital imaginal  
594 discs. *Development* 124, 205–218.
- 595 Cheng, L.E., Song, W., Looger, L.L., Jan, L.Y., Jan, Y.N., 2010. The Role of the TRP Channel  
596 NompC in *Drosophila* Larval and Adult Locomotion. *Neuron* 67, 373–380.  
597 <https://doi.org/10.1016/j.neuron.2010.07.004>
- 598 Cini, A., Ioriatti, C., Anfora, G., 2012. A review of the invasion of *Drosophila suzukii* in Europe  
599 and a draft research agenda for integrated pest management. *Bull. Insectology* 65, 149–160.
- 600 Cloonan, K.R., Abraham, J., Angeli, S., Syed, Z., Rodriguez-Saona, C., 2018. Advances in the  
601 chemical ecology of the spotted wing *Drosophila* (*Drosophila suzukii*) and its applications. *J.*  
602 *Chem. Ecol.* 44, 922–939. <https://doi.org/10.1007/s10886-018-1000-y>
- 603 Craddock, E.M., Kambysellis, M.P., Franchi, L., Francisco, P., Grey, M., Hutchinson, A., Nanhoo,  
604 S., Antar, S., 2018. Ultrastructural variation and adaptive evolution of the ovipositor in the  
605 endemic Hawaiian *Drosophilidae*. *J. Morphol.* 279, 1725–1752.  
606 <https://doi.org/10.1002/jmor.20884>
- 607 Crava, C.M., Ramasamy, S., Ometto, L., Anfora, G., Rota-Stabelli, O., 2016. Evolutionary insights  
608 into taste perception of the invasive pest *Drosophila suzukii*. *G3 Genes, Genomes, Genet.* 6,  
609 4185–4196. <https://doi.org/10.1534/g3.116.036467>
- 610 Erler, G., 1983. Reduction of mechanical sensitivity in an insect mechanoreceptor correlated with  
611 destruction of its tubular body. *Cell Tissue Res* 234, 451–61.
- 612 Falk, R., Atidia, J., 1975. Mutation affecting taste perception in *Drosophila melanogaster*. *Nature*  
613 254, 325–326.
- 614 Falk, R., Bleiser-Avivi, N., Atidia, J., 1976. Labella taste organs of *Drosophila melanogaster*. *J.*  
615 *Morphol.* 150, 327–341.
- 616 Ferguson, L.C., Green, J., SurrIDGE, A., Jiggins, C.D., 2011. Evolution of the insect yellow gene

617 family. *Mol. Biol. Evol.* 28, 257–272. <https://doi.org/10.1093/molbev/msq192>

618 Gillespie, P.G., Walker, R.G., 2009. Mechanotransduction by Hair Cells: Models, Molecules, and  
619 Mechanisms. *Nature* 139, 33–44.

620 Gompel, N., Prud'homme, B., Wittkopp, P.J., Kassner, V.A., Carroll, S.B., 2005. Chance caught on  
621 the wing: cis-regulatory evolution and the origin of pigment patterns in *Drosophila*. *Nature*  
622 433, 481–487.

623 Gong, Z., Son, W., Chung, Y.D., Kim, J., Shin, D.W., McClung, C.A., Lee, Y., Lee, H.W., Chang,  
624 D.J., Kaang, B.K., Cho, H., Oh, U., Hirsh, J., Kernan, M.J., Kim, C., 2004. Two  
625 interdependent TRPV channel subunits, inactive and nanchung, mediate hearing in *Drosophila*.  
626 *J. Neurosci.* 24, 9059–9066. <https://doi.org/10.1523/JNEUROSCI.1645-04.2004>

627 Göpfert, M.C., Albert, J.T., Nadrowski, B., Kamikouchi, A., 2006. Specification of auditory  
628 sensitivity by *Drosophila* TRP channels. *Nat. Neurosci.* 9, 999–1000.  
629 <https://doi.org/10.1038/nn1735>

630 Gorczyca, D.A., Younger, S., Meltzer, S., Kim, S.E., Cheng, L., Song, W., Lee, H.Y., Jan, L.Y.,  
631 Jan, Y.N., 2014. Identification of Ppk26, a DEG/ENaC Channel Functioning with Ppk1 in a  
632 Mutually Dependent Manner to Guide Locomotion Behavior in *Drosophila*. *Cell Rep.* 9, 1446–  
633 1458. <https://doi.org/10.1016/j.celrep.2014.10.034>

634 Grabherr, M.G., Haas, B.J., Yassour, M., Levin, J.Z., Thompson, D.A., Amit, I., Adiconis, X., Fan,  
635 L., Raychowdhury, R., Zeng, Q., Chen, Z., Mauceli, E., Hacohen, N., Gnirke, A., Rhind, N., di  
636 Palma, F., Birren, B.W., Nusbaum, C., Lindblad-Toh, K., Friedman, N., Regev, A., 2011. Full-  
637 length transcriptome assembly from RNA-Seq data without a reference genome. *Nat.*  
638 *Biotechnol.* 29, 644–52. <https://doi.org/10.1038/nbt.1883>

639 Green, J.E., Cavey, M., Médina Caturegli, E., Aigouy, B., Gompel, N., Prud'homme, B., 2019.  
640 Evolution of Ovipositor Length in *Drosophila suzukii* Is Driven by Enhanced Cell Size  
641 Expansion and Anisotropic Tissue Reorganization. *Curr. Biol.* 29, 2075–2082.e6.  
642 <https://doi.org/10.1016/j.cub.2019.05.020>



643 Guo, Y., Wang, Y., Wang, Q., Wang, Z., 2014. The Role of PPK26 in *Drosophila* Larval  
644 Mechanical Nociception. *Cell Rep.* 9, 1183–1190. <https://doi.org/10.1016/j.celrep.2014.10.020>

645 Guo, Y., Wang, Y., Zhang, W., Meltzer, S., Zanini, D., Yu, Y., Li, J., Cheng, T., Guo, Z., Wang,  
646 Q., Jacobs, J.S., Sharma, Y., Eberl, D.F., Göpfert, M.C., Jan, L.Y., Jan, Y.N., Wang, Z., 2016.  
647 Transmembrane channel-like (*tmc*) gene regulates *Drosophila* larval locomotion. *Proc. Natl.*  
648 *Acad. Sci. U. S. A.* 113, 7243–7248. <https://doi.org/10.1073/pnas.1606537113>

649 Hall, T., 1999. BioEdit: a user-friendly biological sequence alignment editor and analysis program  
650 for Windows 95/98/NT. *Nucleic Acids Symp. Ser.* 41, 95–98. [https://doi.org/citeulike-article-](https://doi.org/citeulike-article-id:691774)  
651 [id:691774](https://doi.org/citeulike-article-id:691774)

652 Hauser, M., 2011. A historic account of the invasion of *Drosophila suzukii* (Matsumura) (Diptera:  
653 *Drosophilidae*) in the continental United States, with remarks on their identification. *Pest*  
654 *Manag. Sci.* 67, 1352–1357. <https://doi.org/10.1002/ps.2265>

655 Hickner, P. V., Rivaldi, C.L., Johnson, C.M., Siddappaji, M., Raster, G.J., Syed, Z., 2016. The  
656 making of a pest: Insights from the evolution of chemosensory receptor families in a  
657 pestiferous and invasive fly, *Drosophila suzukii*. *BMC Genomics* 17, 1–17.  
658 <https://doi.org/10.1186/s12864-016-2983-9>

659 Hu, Y., Wang, Z., Liu, T., Zhang, W., 2019. Piezo-like Gene Regulates Locomotion in *Drosophila*  
660 Larvae. *Cell Rep.* 26, 1369-1377.e4. <https://doi.org/10.1016/j.celrep.2019.01.055>

661 Ioriatti, C., Walton, V., Dalton, D., Anfora, G., Grassi, A., Maistri, S., Mazzoni, V., 2015.  
662 *Drosophila suzukii* (Diptera: *Drosophilidae*) and Its Potential Impact to Wine Grapes During  
663 Harvest in Two Cool Climate Wine Grape Production Regions. *J. Econ. Entomol.* 108, 1148–  
664 1155. <https://doi.org/10.1093/jee/fov042>

665 Jang, W., Lee, S., Choi, S.I., Chae, H.S., Han, J., Jo, H., Hwang, S.W., Park, C.S., Kim, C., 2019.  
666 Impairment of proprioceptive movement and mechanical nociception in *Drosophila*  
667 *melanogaster* larvae lacking *Ppk30*, a *Drosophila* member of the Degenerin/Epithelial Sodium  
668 Channel family. *Genes, Brain Behav.* 18, 1–8. <https://doi.org/10.1111/gbb.12545>

- 669 Johnson, B.R., Atallah, J., Plachetzki, D.C., 2013. The importance of tissue specificity for RNA-  
670 seq: Highlighting the errors of composite structure extractions. *BMC Genomics* 14, 1.  
671 <https://doi.org/10.1186/1471-2164-14-586>
- 672 Joseph, R.M., Carlson, J.R., 2015. *Drosophila* Chemoreceptors: A Molecular Interface Between the  
673 Chemical World and the Brain. *Trends Genet.* 31, 683–695.  
674 <https://doi.org/10.1016/j.tig.2015.09.005>
- 675 Kaessmann, H., 2010. Origins, evolution, and phenotypic impact of new genes. *Genome Res.* 20,  
676 1313–1326. <https://doi.org/10.1101/gr.101386.109>
- 677 Karageorgi, M., Bräcker, L.B., Lebreton, S., Minervino, C., Cavey, M., Siju, K.P., Grunwald  
678 Kadow, I.C., Gompel, N., Prud'homme, B., 2017. Evolution of Multiple Sensory Systems  
679 Drives Novel Egg-Laying Behavior in the Fruit Pest *Drosophila suzukii*. *Curr. Biol.* 27, 847–  
680 853. <https://doi.org/10.1016/j.cub.2017.01.055>
- 681 Karkali, K., Martin-Blanco, E., 2017. Mechanosensing in the *Drosophila* nervous system. *Semin.*  
682 *Cell Dev. Biol.* 71, 22–29. <https://doi.org/10.1016/j.semcd.2017.06.014>
- 683 Keil, T.A., Steinbrecht, A.R., 1984. Mechanosensitive and olfactory sensilla of insects, in: Akai,  
684 H., King, R.C. (Eds.), *Insect Ultrastructure, Volume 2*. Springer, pp. 477–516.
- 685 Kernan, M.J., 2007. Mechanotransduction and auditory transduction in *Drosophila*. *Pflugers Arch.*  
686 *Eur. J. Physiol.* 454, 703–720. <https://doi.org/10.1007/s00424-007-0263-x>
- 687 Kim, S.E., Coste, B., Chadha, A., Cook, B., Patapoutian, A., 2012. The role of *Drosophila* Piezo in  
688 mechanical nociception. *Nature* 483, 209–212. <https://doi.org/10.1038/nature10801>
- 689 Kinjo, H., Kunimi, Y., Ban, T., Nakai, M., 2013. Oviposition Efficacy of *Drosophila suzukii*  
690 (Diptera: Drosophilidae) on Different Cultivars of Blueberry. *J. Econ. Entomol.* 106, 1767–  
691 1771. <https://doi.org/10.1603/ec12505>
- 692 Langmead, B., Salzberg, S.L., 2012. Fast gapped-read alignment with Bowtie 2. *Nat. Methods* 9,  
693 357–359. <https://doi.org/10.1038/nmeth.1923>
- 694 Lee, H., Choi, H.W., Zhang, C., Park, Z.Y., Kim, Y.J., 2016. A pair of oviduct-born Pickpocket

695 neurons important for egg-laying in *Drosophila melanogaster*. *Mol. Cells* 39, 573–579.  
696 <https://doi.org/10.14348/molcells.2016.0121>

697 Lee, J.C., Bruck, D.J., Curry, H., Edwards, D., Haviland, D.R., Van Steenwyk, R.A., Yorgey, B.M.,  
698 2011. The susceptibility of small fruits and cherries to the spotted-wing drosophila, *Drosophila*  
699 *suzukii*. *Pest Manag. Sci.* 67, 1358–1367. <https://doi.org/10.1002/ps.2225>

700 Li, B., Dewey, C.N., 2011. RSEM: accurate transcript quantification from RNA-Seq data with or  
701 without a reference genome. *BMC Bioinformatics* 12, 323. [https://doi.org/10.1186/1471-2105-](https://doi.org/10.1186/1471-2105-12-323)  
702 12-323

703 Marshall, K.L., Lumpkin, E.A., 2012. The molecular basis of mechanosensory transduction, in:  
704 Lopez-Larrea, C. (Ed.), *Sensing in Nature*. pp. 142–155.

705 Mi, H., Huang, X., Muruganujan, A., Tang, H., Mills, C., Kang, D., Thomas, P.D., 2017.  
706 PANTHER version 11: Expanded annotation data from Gene Ontology and Reactome  
707 pathways, and data analysis tool enhancements. *Nucleic Acids Res.* 45, D183–D189.  
708 <https://doi.org/10.1093/nar/gkw1138>

709 Muto, L., Kamimura, Y., Tanaka, K.M., Takahashi, A., 2018. An innovative ovipositor for niche  
710 exploitation impacts genital coevolution between sexes in a fruit-damaging *Drosophila*. *Proc.*  
711 *R. Soc. B Biol. Sci.* 285, 20181635. <https://doi.org/10.1098/rspb.2018.1635>

712 Naccarati, C., Audsley, N., Keen, J.N., Kim, J.H., Howell, G.J., Kim, Y.J., Isaac, R.E., 2012. The  
713 host-seeking inhibitory peptide, Aea-HP-1, is made in the male accessory gland and  
714 transferred to the female during copulation. *Peptides* 34, 150–157.  
715 <https://doi.org/10.1016/j.peptides.2011.10.027>

716 Oliveros, J.C., 2015. Venny. An interactive tool for comparing lists with Venn’s diagrams [WWW  
717 Document]. URL <http://bioinfogp.cnb.csic.es/tools/venny/index.html>

718 Ramasamy, S., Ometto, L., Crava, C.M., Revadi, S., Kaur, R., Horner, D., Pisani, D., Dekker, T.,  
719 Anfora, G., Rota-Stabelli, O., 2016. The evolution of olfactory gene families in *Drosophila* and  
720 the genomic basis of chemical-ecological adaptation in *Drosophila suzukii*. *Genome Biol.*

721 Evol. 8, 2297–2311. <https://doi.org/10.1093/gbe/evw160>

722 Sato, K., Tanaka, K., Touhara, K., 2011. Sugar-regulated cation channel formed by an insect  
723 gustatory receptor. *Proc. Natl. Acad. Sci. U. S. A.* 108, 11680–11685.  
724 <https://doi.org/10.1073/pnas.1019622108>

725 Schindelin, J., Arganda-Carreras, I., Frise, E., Kaynig, V., Longair, M., Pietzsch, T., Preibisch, S.,  
726 Rueden, C., Saalfeld, S., Schmid, B., Tinevez, J.-Y., White, D.J., Hartenstein, V., Eliceiri, K.,  
727 Tomancak, P., Cardona, A., 2012. Fiji: an open-source platform for biological-image analysis.  
728 *Nat. Methods* 9, 676–682. <https://doi.org/10.1038/nmeth.2019>

729 Shearer, P.W., West, J.D., Walton, V.M., Brown, P.H., Svetec, N., Chiu, J.C., 2016. Seasonal cues  
730 induce phenotypic plasticity of *Drosophila suzukii* to enhance winter survival. *BMC Ecol.*  
731 <https://doi.org/10.1186/s12898-016-0070-3>

732 Stocker, R.F., 1994. The organization of the chemosensory system in *Drosophila melanogaster*: a  
733 review. *Cell Tissue Res.* 275, 3–26. <https://doi.org/10.1007/BF00305372>

734 Tabarean, I. V., Morris, C.E., 2002. Membrane stretch accelerates activation and slow inactivation  
735 in Shaker channels with S3-S4 linker deletions. *Biophys. J.* 82, 2982–2994.  
736 [https://doi.org/10.1016/S0006-3495\(02\)75639-7](https://doi.org/10.1016/S0006-3495(02)75639-7)

737 Taylor, B.J., 1989a. Sexually dimorphic neurons of the terminalia of *drosophila melanogaster*: II.  
738 Sex-specific axonal arborizations in the central nervous system. *J. Neurogenet.* 5, 193–213.  
739 <https://doi.org/10.3109/01677068909066208>

740 Taylor, B.J., 1989b. Sexually dimorphic neurons in the terminalia of *drosophila melanogaster*: I.  
741 Development of sensory neurons in the genital disc during metamorphosis. *J. Neurogenet.* 5,  
742 173–192. <https://doi.org/10.3109/01677068909066207>

743 Tracey, W.D., Wilson, R.I., Laurent, G., Benzer, S., 2003. *painless*, a *Drosophila* Gene Essential for  
744 Nociception. *Cell* 113, 261–273.

745 Tsubouchi, A., Caldwell, J.C., Tracey, W.D., 2012. Dendritic filopodia, ripped pocket, NOMPC,  
746 and NMDARs contribute to the sense of touch in *Drosophila* larvae. *Curr. Biol.* 22, 2124–

747 2134. <https://doi.org/10.1016/j.cub.2012.09.019>

748 Tuthill, J.C., Wilson, R.I., 2016. Mechanosensation and Adaptive Motor Control in Insects. *Curr.*  
749 *Biol.* 26, R1022–R1038. <https://doi.org/10.1016/j.cub.2016.06.070>

750 Walker, R.G., Willingham, A.T., Zuker, C.S., 2000. Drosophila Mechanosensory Transduction  
751 Channel. *Science* (80-. ). 287, 2229–2234.

752 Zhong, L., Hwang, R.Y., Tracey, W.D., 2010. Pickpocket Is a DEG/ENaC Protein Required for  
753 Mechanical Nociception in Drosophila Larvae. *Curr. Biol.* 20, 429–434.  
754 <https://doi.org/10.1016/j.cub.2009.12.057>

755